Equivalent volume-averaged light scattering behavior of randomly inhomogeneous dielectric spheres in the resonant range

Zhigang Chen and Allen Taflove

Department of Electrical and Computer Engineering, Northwestern University, Evanston, Illinois 60208

Vadim Backman

Department of Biomedical Engineering, Northwestern University, Evanston, Illinois 60208

Finite-difference time-domain numerical experiments and supporting analyses demonstrate that the spectral dependence of the total scattering cross sections of randomly inhomogeneous dielectric spheres of sizes in the resonant range closely resemble those of their homogeneous counterparts that have a volume-averaged refractive index. This result holds even for the extreme case in which the refractive index within an inhomogeneous sphere varies randomly over the range 1.0–2.0. © 2003 Optical Society of America

OCIS codes: 290.5850, 290.0290.

The physical basis and phenomenology of light scattering by particles in the resonant range are of interest in a variety of science and engineering disciplines.[1,2] It is well known that scattering by homogeneous or layered spheres that comprise isotropic dielectrics can be analyzed by Mie theory and its extensions.[2,3] However, because most particles of interest have neither spherical shapes nor homogeneous compositions, their scattering properties cannot be obtained analytically.

In this Letter we report the application of a finite-difference time-domain (FDTD) method[4] to investigate the role that random dielectric inhomogeneities play in light scattering by resonant spheres. Previously, the FDTD showed promise in calculation of scattering by realistic particles because of its ability to model complex surface shapes and internal structures.[5,6] In this Letter we also report an approximate analysis that supports our numerical findings.

First we verified our FDTD code by computing the scattering pattern of homogeneous spheres and comparing the results with Mie theory. A Gaussian pulse wave source was imposed on the simulation grid, and the scattered-field frequency response was extracted by means of a discrete Fourier transform run concurrently with the FDTD time stepping.[4] The perfectly matched layer absorbing boundary condition[7] was used in our simulations to terminate the computational lattice. We constructed a 5-μm inhomogeneous spherical dielectric particle within a FDTD space lattice that had a uniform cubic cell size of 25 nm on a side. Two cases of random inhomogeneity within the particle were studied. In case 1 we assigned a uniformly distributed, fine-grained, random value of permittivity to each lattice cell within the sphere (correlation length, $L_c = 25$ nm). In case 2 we assigned a uniformly distributed, coarse-grained, random value of permittivity to cubic blocks of size $4 \times 4 \times 4$ lattice cells ($L_c = 100$ nm) within the sphere. For both of these cases we calculated the total scattering cross section (TSCS) for an incident wavelength range of

500–1000 nm for two ranges of randomly assigned refractive index, 1.45–1.55 and 1.0–2.0, separately, using a pseudouniform random-number generator.[8]

Figure 1 illustrates typical assignments of the randomly distributed refractive index along a cut through the center of the particle for cases 1 [Fig. 1(a)] and 2 [Fig. 1(b)]. Note that groupings of adjacent random refractive indices create composite internal inhomogeneities with effective length scales that vary over a wide range, as illustrated by the arrows.

Figure 2(a) graphs the FDTD-calculated TSCS (in units of square meters) versus wavelength for 10 random sequences of refractive index ranging from 1.45 to 1.55 for case 1, the fine-grained inhomogeneity. The filled circles represent the results of the FDTD simulations for distinct sets of random inhomogeneities at 30 wavelengths from 500 to 1000 nm. In addition, Fig. 2(a) shows the results of two finer-frequency-resolution FDTD simulations at 30 wavelengths from 750 to 800 nm and at 30 wavelengths from 850 to 900 nm for a single set of random inhomogeneities. For comparison, the dotted curve shows the corresponding Mie data for a 5-μm homogeneous sphere with $n = 1.5$ (the volume average of the random refractive indices of the FDTD runs). From Fig. 2(a) we see that the TSCS of each randomly inhomogeneous particle as a function of wavelength has an oscillatory pattern that closely resembles that of its volume-averaged Mie counterpart. The primary difference is that the FDTD-modeled sphere lacks the high-frequency ripple structure calculated by use of the Mie series. Based on our numerical experiments with extremely fine frequency resolution, we believe that this discrepancy arises from the staircasing of the sphere surface within the FDTD space grid, which reduces the surface-wave effects required for the appearance of the ripple structure.

Figure 2(b) repeats the study of Fig. 2(a) for case 2, the coarse-grained inhomogeneity. Five random sequences of refractive index ranging from 1.45 to 1.55 are examined. Figure 2(b) also shows the results
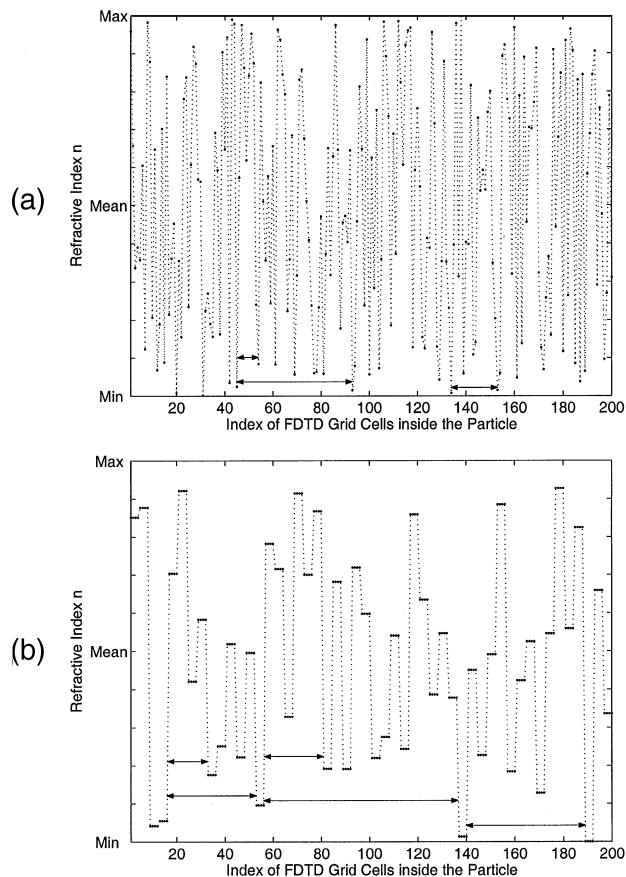
Fig. 1. Typical assignment of randomly distributed refractive indices along a cut through the center of the 5-μm spherical particle; each FDTD grid cell has a size of 25 nm: (a) fine-grained and (b) coarse-grained inhomogeneity.

of a finer-frequency-resolution FDTD simulation at 30 wavelengths from 750 to 800 nm for a single set of random inhomogeneities. Comparing Figs. 2(a) and 2(b), we can see that the primary effect of the coarse-grained inhomogeneity is to slightly broaden the spread of the TSCS. The TSCS of each randomly inhomogeneous particle retains an oscillatory pattern that closely resembles that of its volume-averaged Mie counterpart.

Figure 3 repeats the studies of Fig. 2 for a much wider range of random refractive index, $1.0 \leq n \leq 2.0$, within the inhomogeneous sphere. Here, two sequences of random refractive index in this range were studied for each of cases 1 and 2. It is evident that the TSCS of the randomly inhomogeneous particle as a function of wavelength still resembles that of its homogeneous volume-averaged Mie counterpart, although not so well as previously, especially for the coarse-grained case 2 below 600 nm.

To complement the numerical experiments, we present an analysis of how the internal inhomogeneities of a dielectric particle affect the wavelength dependence of its TSCS. The TSCS of a particle much larger than the incident wavelength can be estimated by the Wentzel–Kramers–Brillouin technique[9] when $(n - 1)kd \gg 1$ and $(n - 1) < 1$, where k is the incident wave number and n and d are

the refractive index and the size of the particle, respectively. In this approximation, the scattering contribution due to surface effects is neglected. To improve accuracy, one can represent TSCS σ_s as the sum of two terms: $\sigma_s = \sigma_s^{(\nu)} + \sigma_s^{(s)}$, where $\sigma_s^{(\nu)}$ is the contribution due to the volume of the scattering particle and $\sigma_s^{(s)}$ is the so-called edge term,[10] which account for the effect of the sharp discontinuity of the refractive index at the particle surface. For a spherical particle of diameter d, $\sigma_s^{(s)}$ can be approximated as $\sigma_s^{(s)} \approx 2\pi(d/2)^2 (kd/2)^{-2/3}$ (where high-frequency ripple structure has been neglected), whereas $\sigma_s^{(\nu)}$ is written as

$$\sigma_s^{(\nu)} = 2 \, \mathrm{Re}\left(\iint_A \{1 - \exp[i\xi(\mathbf{r})]\} \mathrm{d}^2\mathbf{r} \right), \quad (1)$$

where $\mathbf{r}$ is a vector in the plane orthogonal to the direction of propagation of the incident wave; $\xi(\mathbf{r}) = \int_{L(\mathbf{r})} k[nl(\mathbf{r}) - 1]\mathrm{d}l$, in which the integration is performed over the path $L = d[1 - \sin^2 \gamma(\mathbf{r})/n_0^2]^{1/2}$ of the ray inside the particle; γ is the angle between the incident ray's propagation direction and the radial vector pointing from the center of the particle to the point of entry of the ray into the particle; and A is the geometrical cross-section area
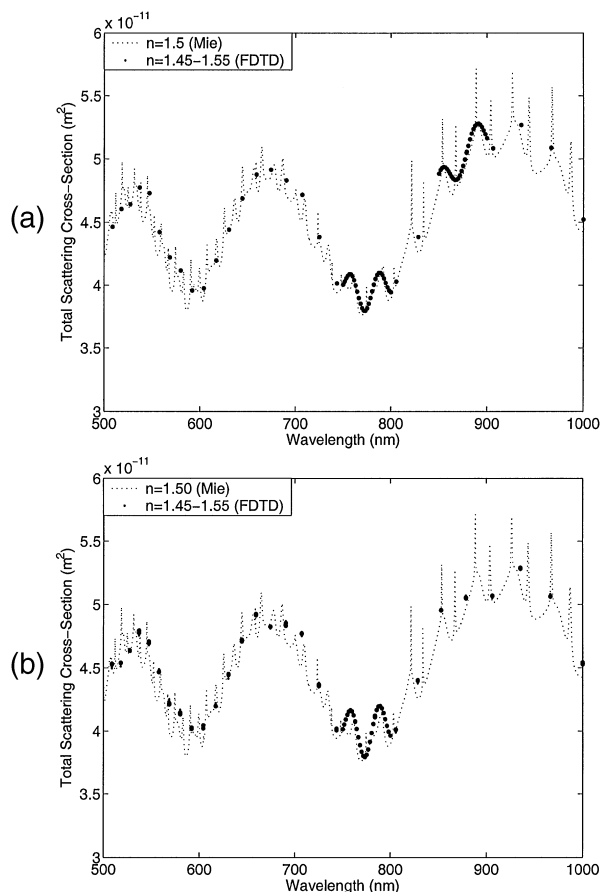

Fig. 2. Total scattering cross section versus wavelength for $1.45 \leq n \leq 1.55$. The ten FDTD simulations are represented by filled circles; the corresponding Mie result, by a dotted curve: (a) fine-grained and (b) coarse-grained inhomogeneity.
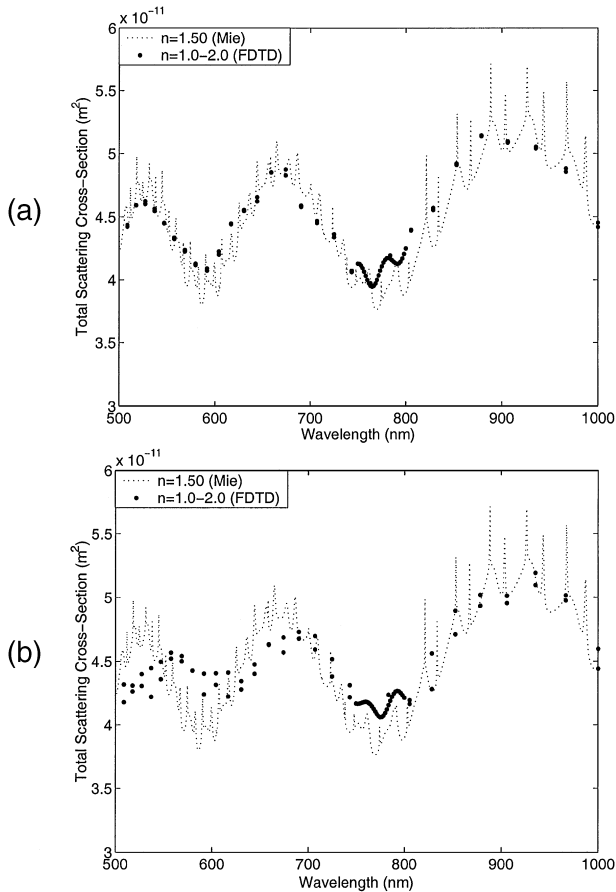
Fig. 3. Total scattering cross section versus wavelength for $1.0 \leq n \leq 2.0$. The two FDTD simulations are represented by the filled circles; corresponding Mie result, by a dotted curve: (a) fine-grained (b) coarse-grained inhomogeneity.

of the particle. The refractive index inside the particle can be written as the sum of mean refractive index n_0 and its spatially varying component $\delta n(\mathbf{r})$: $n(\mathbf{r}) = n_0 + \delta n(\mathbf{r})$. Using this definition and substituting $\xi(\mathbf{r})$ into Eq. (1), we obtain $\sigma_s^{(\nu)} = \pi d^2$ Re $\int_{t^2+n_0^2-1=0}^{t^2+n_0^2-1=n_0} t\{1 - \exp[i(\rho/n_0)(t^2 + n_0^2 - 1)^{1/2}]\exp[i\rho\,\alpha(\mathbf{r})t]\}dt$, where $t = \cos\gamma$, $\rho = kd(n_0 - 1)$, and $\alpha(\mathbf{r}) = [\int_{L(\mathbf{r})} \delta n(\mathbf{r})/(n_0 - 1)dl/d$. If $|\rho\alpha| \ll 1$, the second exponent in $\sigma_s^{(\nu)}$ can be expanded to allow the integration to be performed analytically, yielding

$$\sigma_s = 2\pi(d/2)^2\{1 + [2(n_0 - 1)/\rho]^{2/3} - 2n_0 \sin\rho/\rho$$

$$+ 4n_0 \sin^2(\rho/2)/\rho^2 + \beta(\rho)\}, \qquad (2)$$

where $\beta(\rho) = \rho \int_0^1 \alpha t^2 \sin(t\rho)dt$ accounts for the inhomogeneous distribution of the refractive index inside the particle. When $n_0 \to 1$ and $\beta = 0$, Eq. (2) matches the well-known equation derived by van de Hulst[2] for a homogeneous sphere. However, for an arbitrary refractive index, Eq. (2) provides better agreement with the exact Mie solution.

Now assume that the spatial distribution of δn has a correlation length L_c and a probability-density function characterized by a standard deviation $\sigma_{\delta n} = \{\text{var}[\delta n/(n_0 - 1)]\}^{1/2}$. Then $|\beta(\rho)| < \sigma_{\delta n}L_c/d$,

and the deviation of the TSCS from that of the equivalent volume-averaged uniform sphere is negligible, provided that $L_c \ll d/\sigma_{\delta n}$. For example, if the refractive index inside a 5-μm particle varies with equal probability from 1 to 2 for $L_c = 25$ nm, then $|\beta| \leq 10^{-3}$, and the TSCS is expected to closely follow that of the corresponding volume-averaged uniform sphere. This conclusion is supported by FDTD simulations shown in Fig. 3(a). As discussed above, Eq. (2) is valid when $|\rho\alpha| \propto 2\pi(n_0 - 1)\sigma_{\delta n}(L_c d)^{1/2}/\lambda < \pi/2$. This condition can be used to estimate wavelength λ_c below which the frequency of the interference structure may be affected: $\lambda_c \approx 4(n_0 - 1)\sigma_{\delta n}(L_c d)^{1/2}$. For example, if $L_c = 100$ nm, $d = 5$ μm, and the refractive index varies from 1 to 2 with a uniform probability, then $\lambda_c \sim 800$ nm, which is again observed in our FDTD simulations shown in Fig. 3(b). As another example, if the variations of the refractive index have the same correlation length but are limited from 1.45 to 1.55, then the TSCS follows that of the uniform sphere for a wavelength as short as $\lambda_c \sim 80$ nm, i.e., smaller than L_c.

In summary, we have conducted FDTD numerical experiments and supporting analyses to demonstrate that the spectral dependence of the total scattering cross section of randomly inhomogeneous dielectric spheres of size in the resonant range closely resembles that of their homogeneous counterparts that have a volume-averaged refractive index. This result holds even for the extreme case in which the refractive index within an inhomogeneous sphere varies randomly over the range 1.0–2.0.

References

1. M. I. Mishchenko, J. W. Hovenier, and L. D. Travis, *Light Scattering by Nonspherical Particles: Theory, Measurements and Applications* (Academic, San Diego, Calif., 2000).
2. H. C. van de Hulst, *Light Scattering by Small Particles* (Dover, New York, 1981).
3. M. Kerker, *The Scattering of Light* (Academic, New York, 1969).
4. A. Taflove and S. Hagness, *Computational Electrodynamics: The Finite-Difference Time-Domain Method* (Artech House, Boston, Mass., 2000).
5. P. Yang and K. N. Liou, J. Opt. Soc. Am. A **13,** 2072 (1996).
6. A. Dunn and R. Richards-Kortum, IEEE J. Sel. Top. Quantum Electron. **2,** 898 (1996).
7. J.-P. Berenger, J. Comput. Phys. **114,** 185 (1994).
8. W. H. Press, S. A. Teukolsky, W. T. Vetterling, and B. P. Flannery, *Numerical Recipes in FORTRAN 77: The Art of Scientific Computing* (Cambridge U. Press, New York, 1992).
9. A. Ishimaru, *Wave Propagation and Scattering in Random Media* (Academic, New York, 1978).
10. S. A. Ackerman and G. L. Stephens, J. Atmos. Sci. **44,** 1574 (1987).